

Comparative Study of Left Ventricular Low Wall Motion with Scar Tissue Using 4D Left Ventricular Cardiac Images

Chien-Yi Lee¹, Yashbir Singh¹, Michael Friebe², Wei-Chih Hu¹
¹Chung Yuan Christian University, Zhongli District, Taiwan 320
²Otto-von-Guericke-Universität, Magdeburg, Germany
weichihhu@gmail.com; weichihhu@cycu.edu.tw

ABSTRACT

Myocardial contraction affects the cardiovascular pumping system, and helps in the early phase to detect abnormalities of wall motion noninvasively. In this research, we designed a program to characterize regional abnormalities because scar tissue is very difficult to identify in normal cardiac CT images. We created 10 frames of a 3D heart model that contains the long axis as reference for predicting the left ventricular wall motion. We tested our 4D cardiac model with scar tissue using non-invasive cardiac CT images. Here, four subjects (patients) were involved in this study. Subject 1 and 4 are matching the low motion of surgical area with scar tissue area. Subject 2 found fibrous tissue regions (about 40%), compared with the 2SD (Standard Deviation) region. The fibrotic area is completely overlapped with a low-motion region which indicates the fibrotic area has a significant correlation with the low wall motion region. This research evaluates low wall motion of the left ventricle and detection of fibrosis regions.

Keywords: Left ventricular remodeling; myocardial wall motion; Cardiac imaging; Fibrotic tissue; Noninvasive cardiac evaluation;

2 Introduction

Cardiac disease has become a very challenging clinical problem like regional myocardial injury. It is one of the goals of cardiac imaging methods to measure the regional function of the left ventricle (LV). There are many existing techniques to precise and reliable quantitative regional LV function measurements. Most of the standard methods depend on 2D image sequence data [1, 2, 3, 4, 5, 6]. Most of the techniques have been used end-diastolic (ED) and end systolic (ES) image frames. While the LV expansion and LV thickening from region to region is indicative of ischemia [2, 4, 6]. Song and Leahy have performed the dense-field optical flow approach to include fluid flow models using 3D datasets [7]. The Goldgof research group followed a shape matching idea which is similar to ours; though they primarily use Gaussian curvature employing conformal stretching models [8]. Pentland and Terzopoulos have been studying non-rigid motion models, using finite element analysis, which might be useful for cardiac analysis. The Ayache group unified these two approaches to segment and track the object simultaneously [9]. A recently proposed technique is the use of phase contrast MR images to decipher local velocity [10]. However, MR images take a long in acquisition and resolution is less than CT images. This can be integrated to estimate trajectories of individual points over time [11, 12]. Our new

developments could potentially help in curvature estimation, point-wise non-rigid motion tracking, initial quantitative measures of LV motion, thickening, and 3D visualization techniques. The experimental results from real image sequences of multi-phase and multi-slice cardio CT image will be presented, and future research directions will be discussed.

2 Methods

This is a Comparative study of low wall motion with scar tissue using 4D left ventricular cardiac images. The methodology has been grouped into various categories:

Data Extraction

We used Microsoft Windows 7, the 64-bit platform with Intel Celeron CPU G550, memory DDR3 4GB, Visual C ++ 6.0 MFC4.2 for software development and OpenGL library as a tool for the 3D model [13]. Images were obtained from the Philips computerized tomography (CT) instrument provided by the National Institute of Hospital of Yang-Ming University. This study and the informed consent procedure were approved by the Institutional Review Board of National Yang-Ming University Hospital. Each subject has 10 sets of timing frames, including a complete heartbeat cycle. 1 set of 3D cardiac image has 400 slice of cardiac CT images. The scanned image size is 512×512 (pixels). 1 voxel is 0.165 mm^3 ($0.429 \times 0.429 \times 0.9$) where ($x \times y \times z$). We used this images to extract edges of endocardium and estimated the endocardium area of LV. In this way, we find the change of edges of wall motion.

The program flow is as follows:

- Read the image into the program, confirm the format for the DICOM (Digital Imaging and Communications in Medicine), the image is 512x512gray form stored in the program.
- 3D reorganization and image information is obtained to construct the stereoscopic model of the thoracic area. Set the left ventricular central axis and resample the image [13].
- Perform a manual split using our program at the first slice only then use the regional growth law circle, draw the contour of the left ventricular endocardium.
- The endocardial shape of the LV endocardium is magnified at a variable magnification, and the boundary of the second regional growth is made.
- Repeated manual segmentation is performed to obtain epicardial information. 3D model LV endocardium and epicardium is established by a triangular mesh [14, 15].

Left Ventricular Edge Search

We use manually cutting of LV images from base to apical from the entire data set, selected one image from the dataset and one seeded point to start this process. We obtained the geometrical center that connects each slice on long axis, applied regression calculation to find the line as a reference axis for LV [16, 17].

Manually Divide the left Ventricle

In this section, we performed re-sampling of the images to find the short axis, separated LV from aorta (Fig 1).

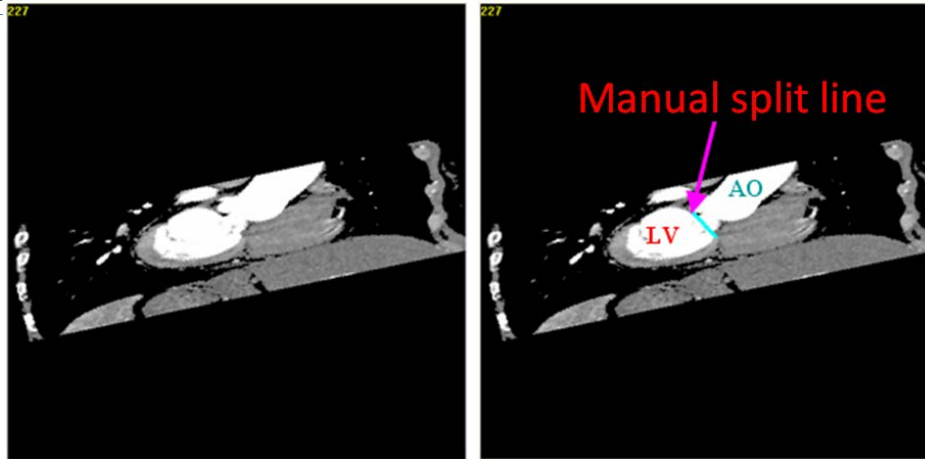


Figure 1. Manually separated line between left ventricle and the aorta.

Regional Growth Circle Selected Endocardium

In this study, the left ventricular endocardial circle is used for the regional growth of the image which is close to the edge of the image. The regional growth of the operation is needed to set up the initial seed point. The initial point of the first slice will be considered as the reference point of the second slice, the second reference point will be set as the seeded region for other layers simultaneously (Fig 2) [16, 17]. It is necessary to confirm that the seeded spots of each layer are in the endometrial region, if not, we need to manually correct the seed points.

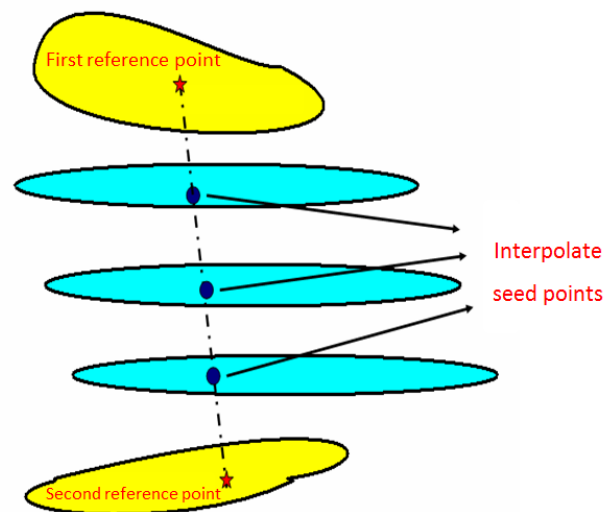


Figure 2. Seeded Point Star from the First Layer and The Last Layer.

Simulation Study

The simulation model is proposed by Yang Bochuan and Ma Minghui. We obtained LV endocardium and the outer membrane Lattice model at different time of the long axis, calculated the diastolic and systolic period of the radius between the rates of change. After that we obtained the number of myocardial changes at each time. These steps are to obtain the simulated left ventricular at each time. This stereoscopic model is to simulate the changes of the LV in the cardiac cycle and the different values of myocardial changes in each block [18].

Triangular Mesh

We use triangular mesh for LV endometrial and adventitial information 3D. The number of samples for the study of 31 layers of each layer of 30 points a total of 930 points, which defines 1 to 10 layers for the base, 11 to 20 layers is the top layer, the 21-30 layers is the middle layer, and the 31st floor is the reference layer. The sampling method divides the total number of the left ventricles by 31 layers, and stores the coordinate points (X, Y, Z). The simulation is to use these 930 points to do the simulation movement. We calculate the momentum information of the heart when the low amount of movement occurs [15, 19].

Simulated Model End of Diastolic Phase

LV contracts at the centre axis. The endometrial and adventitial information goes the left ventricular central axis to establish a triangular mesh model (Fig 3), which shows the gap between outer membrane model and the endometrial model. 10 frame of the triangular mesh is done. In the endometrial triangular mesh model found with the degree of myocardial changes in different levels of red, yellow, green, light blue and dark blue are five colors (Fig.4), and will record the picture in the dark blue block coordinates.

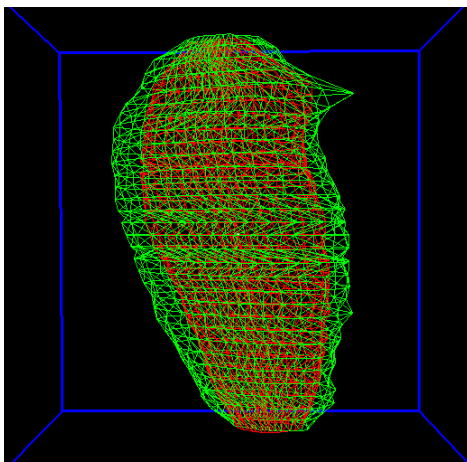


Figure.3 Left Ventricular Triangular Mesh Simulated Model that represents green color for outer membrane model, red for the endometrial model.

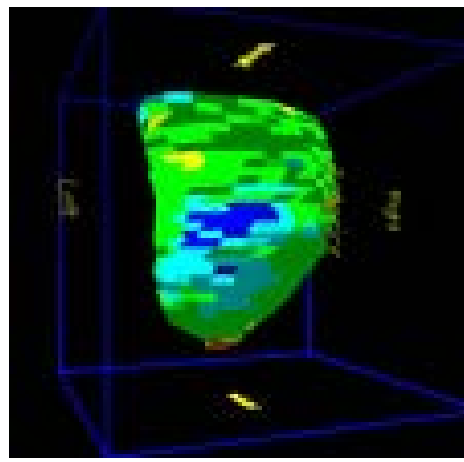


Figure.4 Simulation model of left ventricular motion analysis.

Fibrosis Area Assessment Interface

This study explores the relationship between regional and motion. Hiroaki and other scholars performed the method using patient's delayed-enhancement images that determined the area of fibrotic tissue. This interface exhibit the calculation within the region of the HU (Hounsfield unit) average or press the single click in the block on the right mouse button, point to the center of the circle to 10 points for the radius of the circle. It automatically calculates the circle within the HU average and pink color display in the circular area (Fig.5). We get the region of interest HU value which shows region of fibrosis. This experiment performed to find the fibrosis area [20, 21].

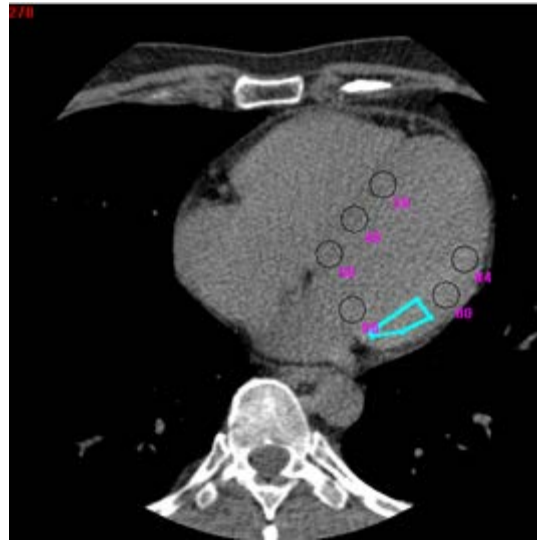


Figure.5 Fibrous area assessment interface (Pink circle area is the HU value of the manual selection area).

3 Results

Motion Model Analysis Interface

We determined 10 lattice grid models in the DICOM 0 timing to reconstruct 3D heart volume and executed the program. We get a 4D model of LV motion. This display interface allows the user to observe the three-dimensional model of the inner portion of the left ventricle (Fig 6). The red color model represents a 3D model of the inner membrane, whereas the green color model represents the three-dimensional model of the outer membrane. This simulation system exhibits the LV outer membrane state of motion (Fig.7) which provides better understanding of the movement of the myocardium in the LV. This method is used dynamically to increase the number of left ventricle models in a linear interpolation method.

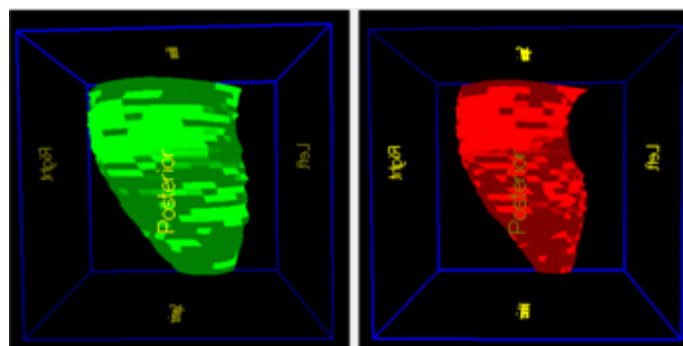


Figure.6 Analog interfaces (The red color model represents inner membrane of 3D, green color model represents outer membrane of 3D).

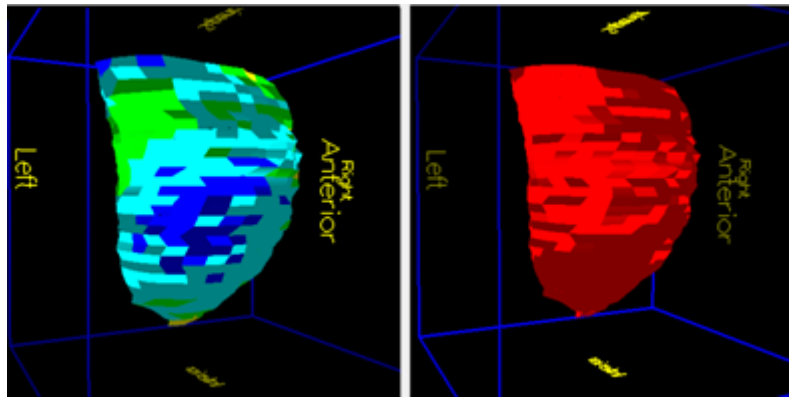


Figure.7 Dynamic interface diagram.

left Ventricular Low Motion Region Assessment

Different color areas represent the difference between the mean left ventricular displacements. The blue is the relative displacement of 2 mm or less, the light blue is the displacement 2 ~ 3 mm, green is the displacement of 3 ~ 4 mm, yellow is the displacement of 4 ~ 5mm, red is the displacement of more than 5mm, and low-motion area is defined as the average amount of difference between the value of less than 2mm area. This study re-sampled after the left ventricular model 1 to 10 layers defined as the base layer, 11 to 20 layers is defined as the middle layer, 21 to 30 layers defined as the top layer. The method takes 30 points of sampling points counterclockwise (Fig. 8) (Fig. 9) (Table. 1).

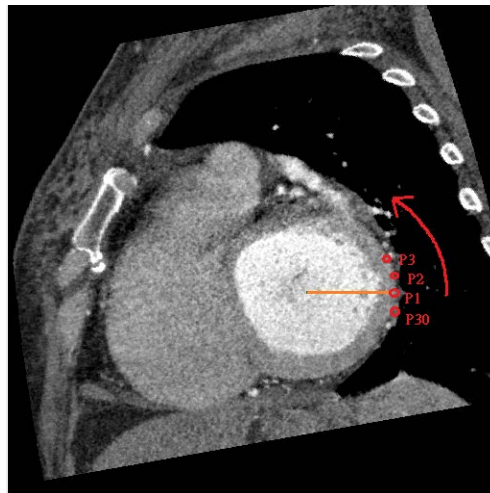
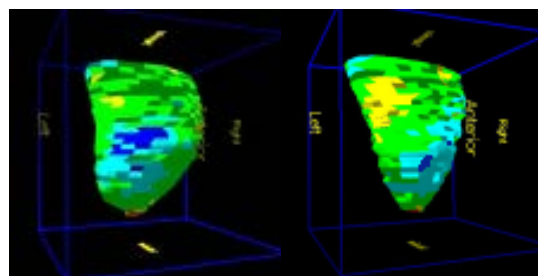
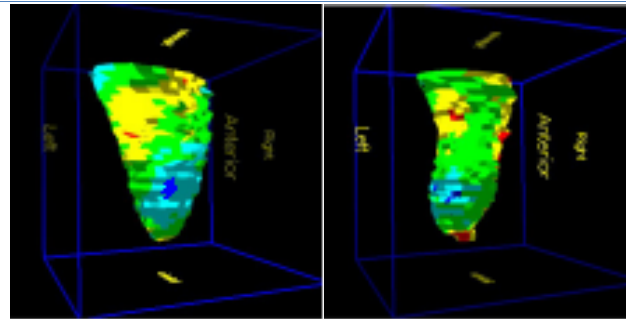


Figure.8 Re-sampling the sampling point.



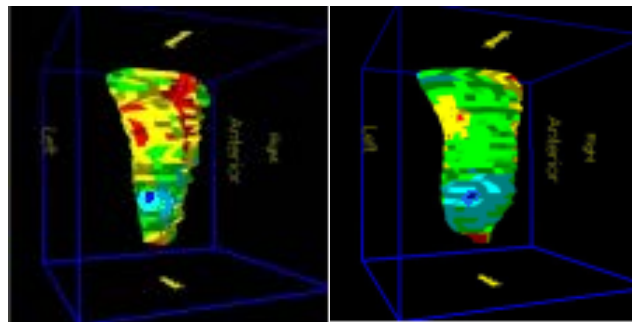
Timing series 0

Timing series 1.



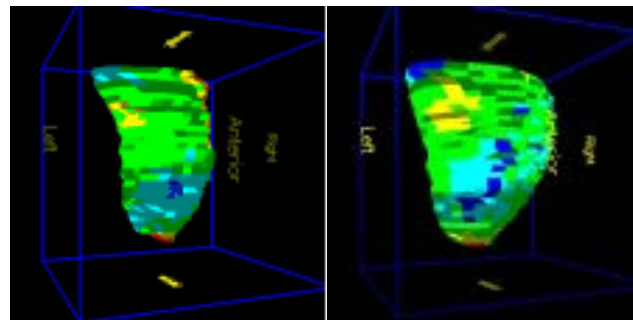
Timing series 2

Timing series 3.



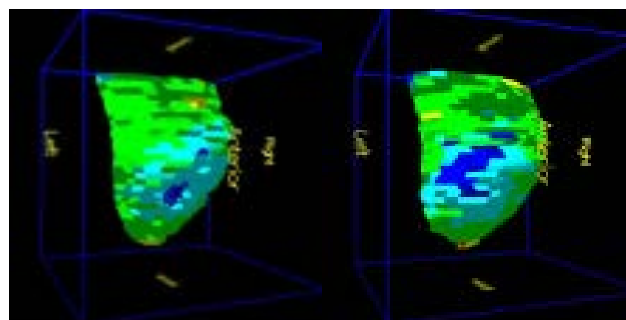
Timing series 4

Timing series 5.



Timing series 6

Timing series 7.



Timing series 8

Timing series 9.

Figure.9 Myocardial changes in the model of subject 1 at every time series.

Table.1 Analysis result

Patients	Generation layer	Segment group location	Point shift	Position evaluation
Subject1	8	Segment 23, Degree 276	1.712mm	Middle layer Posterior side
		Segments 24, Degree 288	1.784mm	
		Segments 23, Degree 276	1.672mm	
	9	Segments 24, 288 degree	1.559mm	
		Segments 25, 300 degree	1.588mm	
		Segments 26, 312 degree	1.576mm	
		Segments 23, 276 degree	1.695mm	
	10	Segments 24, 288 degree	1.701mm	
		Segments 25, 300 degree	1.543mm	
	11	Segments 24, 288 degree	1.728mm	

We observed the low-motion region in the LV (Table .2) and defined 1 to 15 points for the front side (inferior), 16 to 30 points for the back (inferior), each interval is 12 degrees sampling points. In addition, the movement model analysis interface calculated with low sequence (Table.3).

Table. 2 Location of scar tissue in the patients after surgery.

Number of patients	Number of layers	area
Subject1	Middle layer	Posterior side
Subject2	Middle layer	Anterior side, posterior side
Subject3	Lower Layer	Posterior side
Subject4	Lower Layer	Anterior side

Table.3 Detection of the fibrotic tissue location.

No. of Patients	HU (Avg)	(Std Devi)	Greater than 2SD layers	Area
Subject1	60.2	8.4	266~274(middle layer)	Posterior side
Subject2	58.7	7.9	271~283(Middle layer)	Anterior side
Subject3	71.3	12.1	No	no
Subject4	64.5	9.0	302~309(base layer)	Anterior side

Determination of left Ventricular Fibrosis Area

We performed patient's surgery of LV site. Using meglumine diatrizoate, we developed enhancement image criteria using Zeinab et al, found the information of the single image with a fibrotic area, scanned the 10-slice and 20-slice myocardial wall area to ensure that the post-operative area in the left ventricle pattern which is defined by the spinal cord for the posterior Side. It contains the lower wall of the hypopharynx, inferior wall, back wall and front of the spinal cord that contains septal, anterior wall and other blocks. We scan whole heart during the systolic phase and find the area which has low changing radius to match the scar area as low wall motion area. The changing radius is 7.76% which is less than the average changing radius that exhibits low wall motion of LV. The assessment of impaired myocardial function is compared to the central axis angle. Low-motion region is only related to the change in the radius. Therefore, this study shows that the maximum low-motion area, affect the central axis angle changes. The low-volume region is the fibrotic area; results are found (Table. 4).

Table 4. Descriptive result of Subject 1.

Individual	The layer of surgical position	Surgical area	The slice of left ventricle	HU value is greater than the average 2SD area(HU value>77)	Resample the model layer	Point group location	Point group displacement
Subject1	Middle layer	Posterior	266 slice	No	Eleventh	The 23rd point(Degree 276)	1.712mm
			267 slice	No			
			268 slice	Degree 264(HU value85) Degree 276(HU value77) Degree 264(HU value86) Degree 276(HU value92)			
			269 slice	Degree 336(HU value79) Degree 348(HU value77) Degree 264(HU value89) Degree 276(HU value92)		The 24th point(Degree 288)	1.784mm
			270 slice	Degree 288 (HU value83) Degree 312(HU value79) Degree 336(HU value79) Degree 252(HU value80) Degree 264(HU value90)			
			271 slice	Degree 276(HU value83) Degree 348 (HU value78) Degree 324(HU value85) Degree 252(HU value79) Degree 264(HU value84)		The 23rd point(Degree 276)	1.672mm
			272 slice	Degree 336(HU value79) Degree 348(HU value82) Degree 264(HU value84)		The 24rd point(Degree 288)	1.559mm
			273 slice	Degree 276(HU value79) Degree 348(HU value81) Degree 264(HU value80)		The 25rd point(Degree 300)	1.588mm
			274 slice	Degree 276(HU value77) Degree 348(HU value77)		The 26rd point(Degree 312)	1.576mm
			275 slice	No		Ninth	The 23rd point(Degree
276 slice	No						

277 slice	No		276) The 24rd point(Degree 288)	1.701mm
278 slice	No		The 25rd	
279 slice	No		point(Degree 300)	1.543mm
280 slice	No			
281 slice	No			
282 slice	No		The 24th	
283 slice	No	Eighth	point(Degree 288)	1.728mm
284 slice	No			
285 slice	No			

We have four Subjects (Patients), Subject 1 and 4 are matching the low motion of surgical area with scar tissue area. Patient 2 has five districts surgical area, the presence of fibrous tissue is only two regions (about 40%), compared with the 2SD (Standard Deviation) region. The region is higher than the average of 1.6 to 1.8 times the SD value produced. Compared with larger than 2SD region, a slow-motion region found, the fibrotic area completely overlapped with a low-motion region which indicates the fibrotic area. It has a significant correlation with the low-motion region. This study is also found that the fibrosis area is significantly lower than low exercise area. Injured area involved in the movement of adjacent muscles which led to low mobility area than the fibrosis area to the wide. Subject 3 is no fibrotic tissue in this region, as long as the myocardial injury to a certain extent will lead to low motion incidence of the region, but the system can still find the low motion region and position. Only the low-motion area is the medium-risk group in the non-scar area. This study is compared with the fibrotic area method which is proposed by the previous research, our study is to detect the low motion area. It is possible to predict the location of the fibrosis region by irradiating the delayed-enhancement image. The tool can further identify the area of low motion activity without fibrosis, which is performed by the physician for early monitoring, and tracking can provide effective help.

4 Conclusion

This research evaluated low wall motion of the left ventricle of the four patients after surgery, myocardial changes analysis and fibrosis of the region confirms the feasibility of the myocardial movement. This method is sensitive to detect the myocardium dysfunction. We can apply this method to find different types of ventricle disease of the cardiomyopathy. This study is included the assessment of myocardial infarction, Cardiac remodeling and assessing the role of fibrotic tissue in the heart. Further research will involve the integration of the heart motion, validating geometrical landmarks and integration of the motion matching.

REFERENCES

- [1] J. Areeda, E. Garcia, K. Vantrain, D. Brown, A. Waxman and D. Berman. A comprehensive method for automatic analysis of rest/exercise ventricular function from radionuclide angiography. *Digital Imaging: Clinical Advances in Nuclear Medicine*, 1982.
- [2] E. L. Bolson et al. Left ventricular segmental wall motion - A new method using local direction information. *The computer in Cardiology*, 1980.
- [3] I. Clayton et al. The characteristic sequence for the onset of contraction in the normal left ventricle. *Circulation*, 1979, 59:671.

- [4] H. Gelberg et al. Quantitative left ventricular wall motion analysis: A comparison of area, chord, and radical methods. *Circulation*, 1979, 59:991-1000.
- [5] C. Slager et al. Quantitative assessment of regional left ventricular motion using endocardial landmarks. *JA CC*, 1986.
- [6] D. Zisserman et al. Cardiac catheterization and angiographic analysis computer applications. *Progress in Cardiovascular Diseases*, 1983.
- [7] S. Song and R. Leahy. Computation of **3D** velocity fields from **3D** cine CT images. *IEEE Transactions on Medical Imaging*, 1991.
- [8] C. Kambhamettu and D. Goldgof. Point correspondence recovery in non-rigid motion. *IEEE Computer Vision and Pattern Recognition*, 1992, 222- 227.
- [9] A. Pentland and B. Horowitz. Recovery of nonrigid motion and structure. *IEEE Transactions on Pattern Analysis and Machine Intelligence*, 1991.
- [10] D. Terzopoulos and D. Metaxas. Dynamic 3D models with local and global deformations: deformable superquadrics. *IEEE Transactions on Pattern Analysis and Machine Intelligence*, 1991
- [11] N. J. Pelc, A. Shimakawa and G. H. Glover. Phase contrast cine MRI. *Proceedings of the 8th Annual SMRM*, 1989.
- [12] J. van Welden, G. Holmvang, H. Kantor and T. J. Brady. Measurement of myocardial strain with phase sensitive MR. *Proceedings of the 9th Annual SMRM*, 1990.
- [13] W. J. Richard S., "OpenGL Super Bible," 1996.
- [14] Monga and N. Ayache. From voxel to curvature. *IEEE Computer Vision and Pattern Recognition*, 1991, 644-649.
- [15] P. T. Sander and S. W. Zucker. Inferring surface trace and differential structure from **3D** images. *IEEE Transactions on Pattern Analysis and Machine Intelligence*, 1990, 12(9):833-854.
- [16] J. Park, D. Metaxas, A. A. Young, and L. Axel, "Deformable models with parameter functions for cardiac motion analysis from tagged MRI data," *IEEE Transactions on Medical Imaging*, 1996.
- [17] J. Huang, D. Abendschein, V. G. Davila-Roman, and A. A. Amini, "Spatio-temporal tracking of myocardial deformations with a 4-D B-spline model from tagged MRI," *IEEE Transactions on Medical Imaging*, 1999.
- [18] M. F. Smith, "The effect of contraction and twist on myocardial PET and SPECT image resolution: a mathematical phantom study," *IEEE transactions on nuclear science*, 2000.
- [19] L. H. Staib and J. S. Duncan. Deformable Fourier models for surface finding in **3D** images. *SPIE Vol. 1808: Visualization a Biomedical Computing*, 1992.
- [20] Fearmonti, R., Bond, J., Erdmann, D., & Levinson, H. A review of scar scales and scar measuring devices. Eplasty, 2010.
- [21] Razi, T., Niknami, M., & Ghazani, F. A. Relationship between Hounsfield unit in CT scan and grayscale in CBCT. *Journal of dental research, dental clinics, dental prospects*, 2014.